Supporting Information

Paredez et al. 10.1073/pnas.1018593108

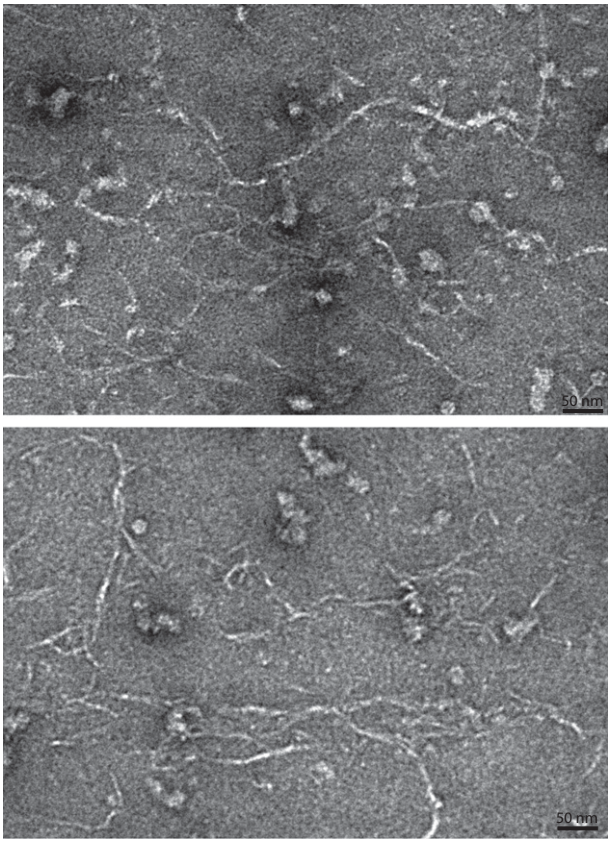

Fig. S1. TEM of negatively stained giActin. Shown are two micrographs of negatively stained giActin filaments. (Scale bar, 50 nm.)

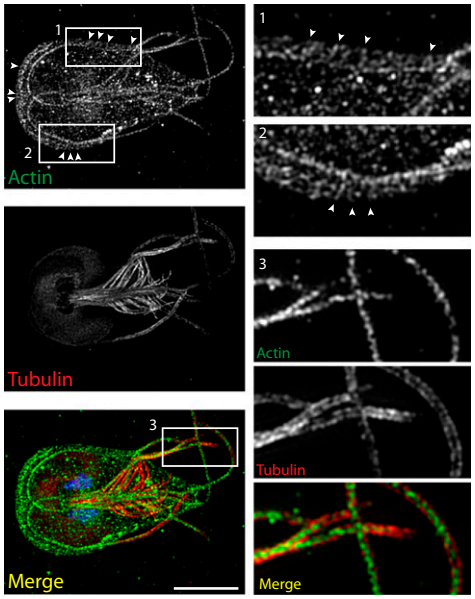

Fig. S2. 3D-SIM analysis of the *Giardia* cytoskeleton. Actin is green, tubulin is red, and DNA is blue. Note that C-shaped filaments are clearly observed all along the side of the trophozoites, indicated by white arrowheads in box 1 and box 2. Also note the repeating zig-zag pattern of actin within the flagellar axoneme, box 3. (Scale bar, 5 μm.)

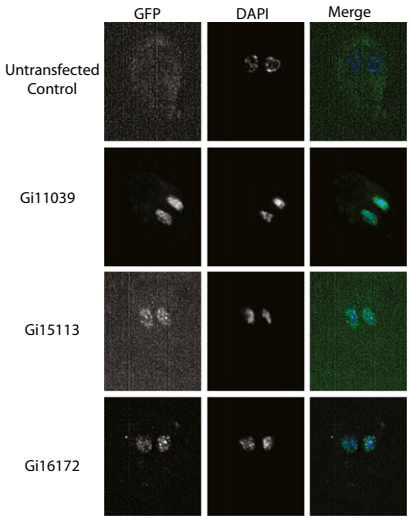

Fig. S3. Localization of the ARPs in *Giardia*. An untransfected control is compared with N-terminal GFP fusions to giARP ORF 11039, 15113, and 16172. All three giARPs are found in the nuclei. GiORF sequences are available from www.giardiadb.org.

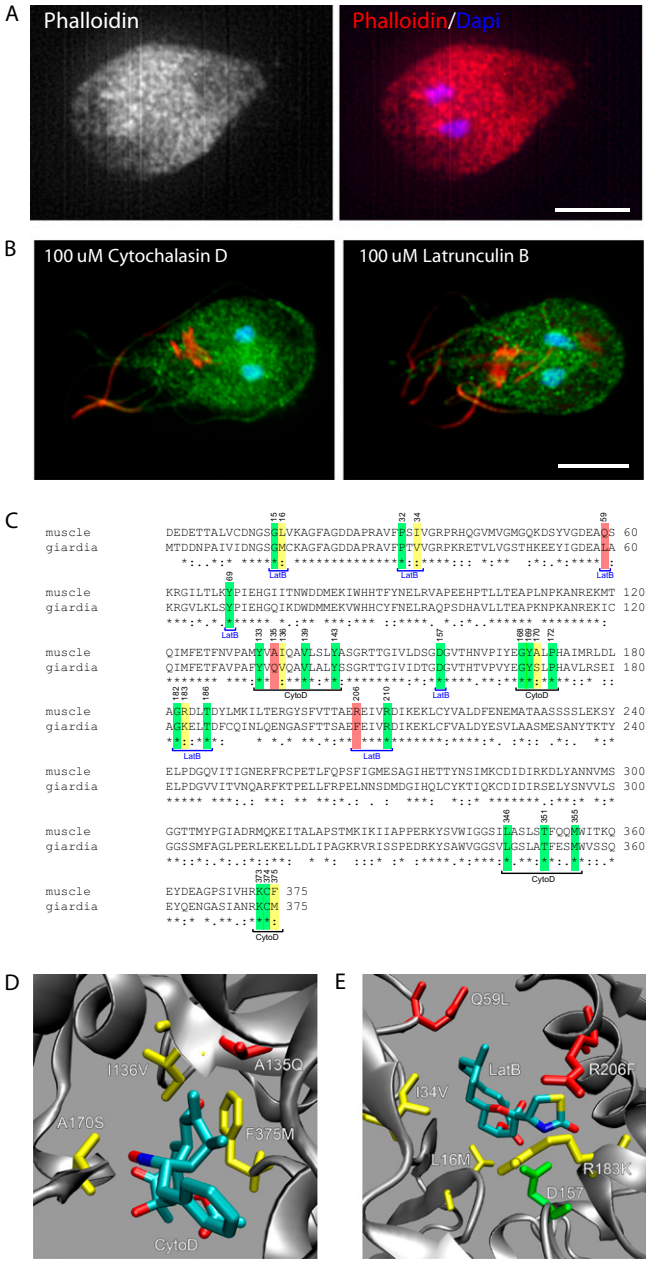

Fig. S4. *Giardia* actin has reduced affinity for phalloidin, cytochalasin D, and latrunculin B. (*A*) Representative *Giardia* trophozoite fixed as in Fig. 2 and stained with rhodamine-phalloidin and DAPI. Note the diffuse staining pattern and the lack of any distinct structure. (*B*) Representative *Giardia* trophozoites exposed to 100 μM cytochalasin D or latrunculin B for 24 h. Actin is in green and tubulin in red. Note overall organization is unaffected by drug treatment. (*C*) Alignment of giActin with muscle actin highlighting key residues for coordinating cytochalasin D and latrunculin A drug binding. Conserved residues are in green, similar residues are in yellow, and nonconservative substitutions are in red. The indicated substitutions are consistent with reduced drug affinity. (*D*) Model of cytochalasin binding. Key residues in the cytochalasin binding pocket have substitutions that are likely to disrupt drug binding. A135 is substituted with a much larger and polar glutamine in giActin. Also, amino acid I36 has been substituted for the smaller valine, and apolar A170 has been substituted for polar serine. (*E*) Model of latrunculin binding. The muscle actin drug-binding pocket has a strong positive density, which is disrupted in *Giardia*. There are also two important polar-to-nonpolar substitutions, R206F and Q59L. Additionally, Q59 normally occupies the same space as bound latrunculin and is thought to move out of position as R206 (F206 in *Giardia*) forms a salt bridge with latrunculin. The substitution R183K sterically blocks D157 from hydrogen bonding to latrunculin, further reducing the likelihood of actin binding. (Scale bar, 5 μm.)

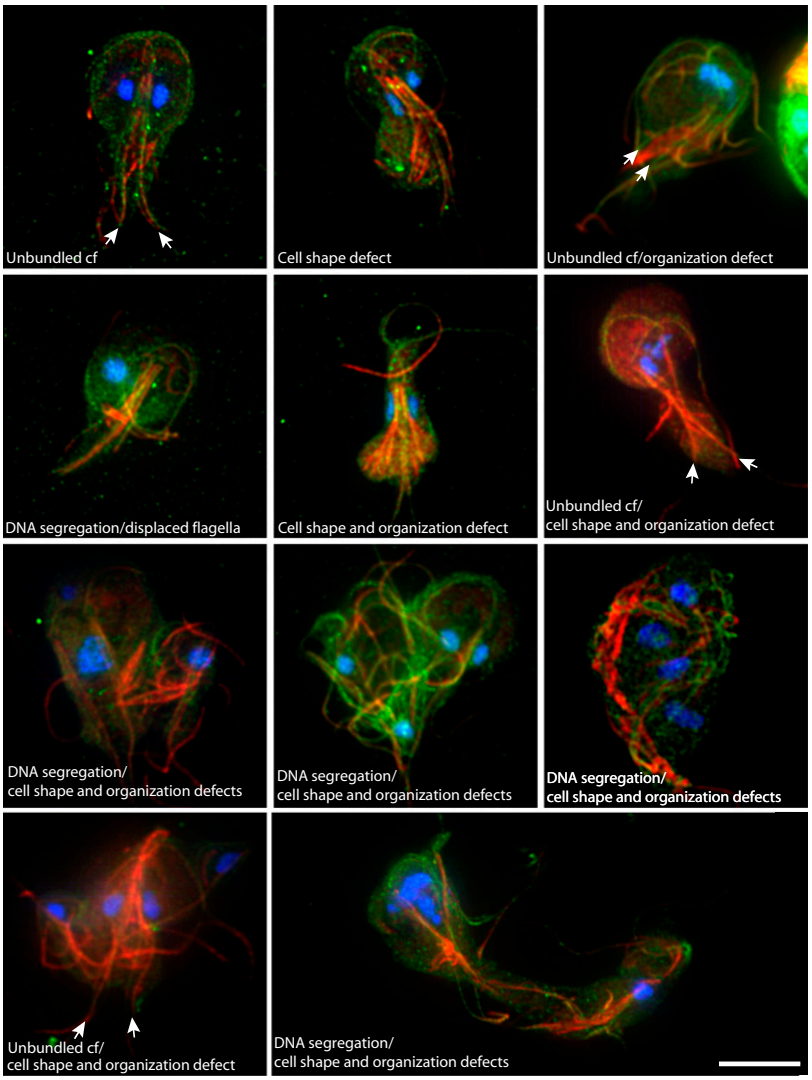

Fig. S5. Additional examples of knockdown phenotypes. Immunofluorescence projections of actin knockdown trophozoites. Actin is green, tubulin is red, and DNA is blue. Arrows indicate unbundled caudal flagella. Note indicated cell shape, polarity, organization, and DNA segregation defects. (Scale bar, 5 μm.)

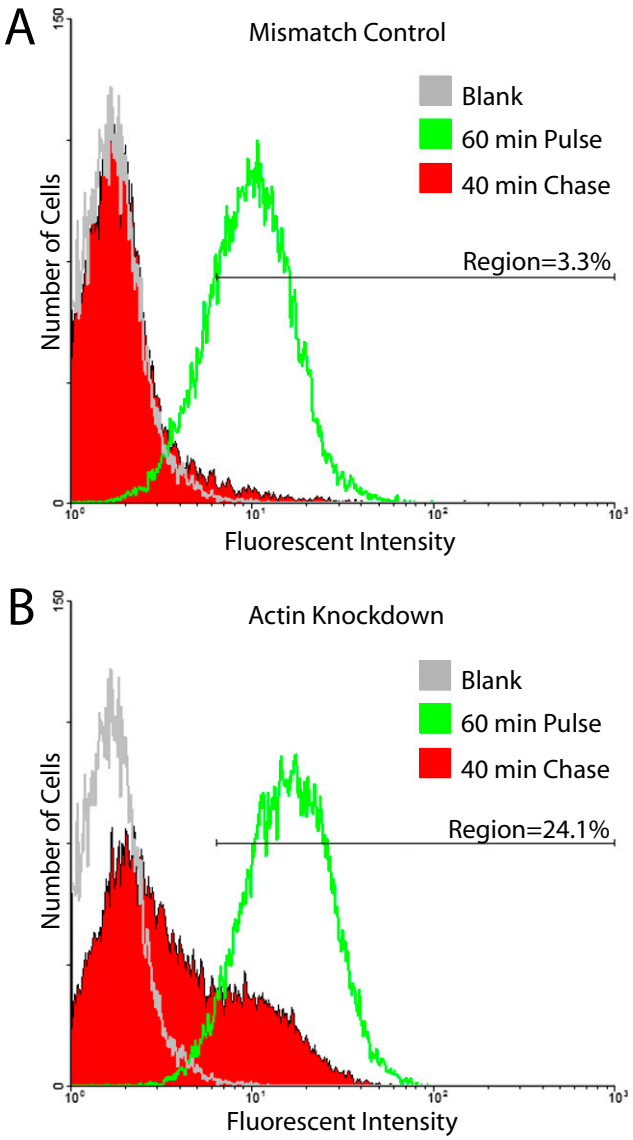

Fig. S6. Actin is required for processing Lucifer yellow subsequent to fluid-phase endocytosis. (*A*) Mismatch control. (*B*) giActin knockdown cells were pulsed with Lucifer yellow for 1 h and chased for 40 min. Treatments were analyzed by flow cytometry. The data shown are representative of the three experimental replicates. Average remaining fluorescence of control experiments is 3.2 ± 1% and average of actin kDa is 30.4 ± 8.6%.

Table S1. List of *Giardia* and *Spironucleus* cytoskeleton components

Microtubule cytoskeleton	*Giardia* ORF	*Spironucleus* (EST cluster)
Centrin	6744; 104685	2917526:1
Dynein heavy chain	16804; 37985; 111950	2915954:1; 2918270:1
Dynein heavy chain	10538; 94440; 40496	2915443:2; 2918316:1
Dynein heavy chain	17478; 101138; 17265	2915443:1; 2917680:1
Dynein heavy chain	17243; 93736; 8172	2918316:2
Dynein heavy chain	100906; 103059; 42285	2918270:2
EB1	14048	Not found
Tubulin alpha	103676; 112079	2916270:6; 2916270:5; 2916270:1; 2916270:2
Tubulin beta	101291; 136020; 136021	2916270:6; 2916270:5; 2916270:1; 2916270:2
Tubulin gamma	114218	2916270:6; 2916270:5; 2916270:1;
Radial spoke protein	16450	Not found
IFT188	16660	Not found
Katanin p60	15368	2916306:1; 2916306:2; 2916245:2; 2916245:1; 2915298:1; 2917083:150
Kinesin-1 (KIF5A)	13825	2917377:1; 2917178:2; 2916192:2; 2918191:1
Kinesin-2 (KIF3A)	16456; 17333,	2917377:1; 2917178:2; 2916192:2; 2918191:1
Kinesin-5 (KIF11)	16425	2916192:2; 2917377:1; 2917178:2; 2918191:1
Kinesin-13 (KIF2A)	16945	2917377:1; 2916192:2; 2917178:2; 2918191:1
Actin cytoskeleton	*Giardia* ORF	*Spironucleus* (EST cluster)
Actin	40817	2916433:1;* 2916973:1;† 2916014:1;† 2916254:15†
Actin-related protein	15113; 16172; 11039	2915520:1‡
ABP1/drebrin	None	Not found
AIP1	None	Not found
Alpha-actinin	None	2915375:3 (coiled coil protein P = 1.3*e*-20)
Capz/capping protein	None	Not found
Clathrin	102108	2915858:8
Coronin	None	Not found
Dynamin	14373	2916220:3; 2916220:2
Cofilin	None	Not found
Dynactin	None	Not found
EPS15	None	Not found
Fimbrin/plastin	None	2915913:2 (matches CH domain P = 1.9*e*-24)
Formin	None	Not found
Gelsolin	None	Not found
Myosin	None	Not found
Profilin	None	Not found
Scar	None	Not found
Tropomyosin	None	Not found
Wasp	None	Not found

The indicated human sequence was blasted against the *Giardia* genome and the *Spironucleus* EST cluster collection. *Giardia* ORF or *Spironucleus* EST cluster hits (P < 1e-15) are listed. Note that tubulin cytoskeleton components and actin are readily identified, whereas none of the core ABPs are found.

*EST encodes for svActin with 58% identity to human actin and 61% identity to giActin.

†Partial sequences, cluster with giActin in phylogenetic analysis.

‡EST with 37% identity to human actin weakly clusters with Arp8.

Table S2. Oligo sequences used in *Materials and Methods*

Oligo	Sequence
pTetGFPn 15113-F	aattaTTCGAAtatgctcgtgccaagcctctc
pTetGFPn 15113-R	aaacgGCGGCCGCtcagaggcgccgcctgtcga
pTetGFPn 16172-F	agtagTTCGAAtatgacactcattcagctccc
pTetGFPn 16172-R	ttttgGCGGCCGCtcacattatcactttcatta
pTetGFPn 11039-F	ctttcTTCGAAtatggatcaaagccgttttgc
pTetGFPn 11039-R	tactcGCGGCCGCttactttgttgccttttccg
GlySer linker F	[Phos]gtacaagtccggaggcggagggagcggcgggggcggaagcgcttcgaattctgcagtcgcgggcccgggatccgc
GlySer linker R	[Phos]ggccgcggatcccgggcccgcgactgcagaattcgaagcgcttccgcccccgccgctccctccgcctccggactt
BestBac-giActin-F	tcccccgggatgtcgtactaccatcacca
BestBac-giActin-R	tttgaattctcacatacacttacg
pET30C(+) giActin-F	atgggatatctgatgacagacgacaaccctgc
pET30C(+) giActin-R	cgcaagctttcacatacacttacggtttg
Rac_NF	atgactagtacaggaaatgaggatac
Rac_CR	CTAGAATATAACACACTTTCCCTTTC
Rac_CA-F	tgcgggccTggaggatta
Rac_CA-R	TAATCCTCCAGGCCCGCA
Actin morpholino	GCAGGGTTGTCGTCTGTCATTTTAC
5x Mis morpholino	GCAcGGTTcTCcTCTGTcATTTaAC

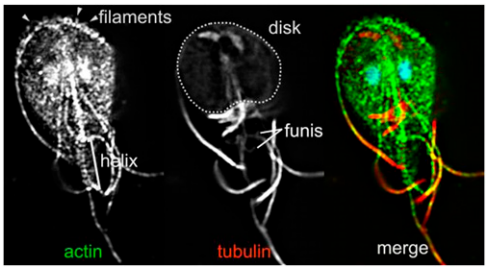

Movie S1. *Z*-series through the interphase trophozoite in Fig. 2. Note the helix bundling the caudal flagella (bracket) and the short filaments along the anterior (arrowheads).

Movie S1

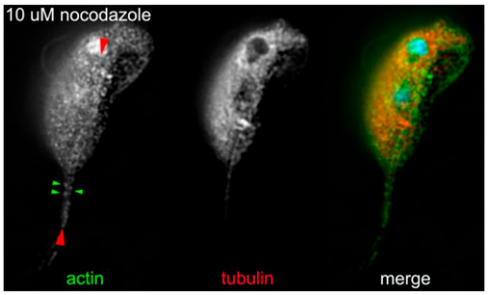

Movie S2. *Z*-series through a trophozoite exposed to 10 μM nocodazole for 6 h. Microtubules are red, actin is green, and DNA is blue. As a result of microtubule depolymerization, the cell rounded up, causing the resistant caudal axonemes to protrude from the cell, improving visibility of the actin helix marked by red arrowheads. Green arrowheads indicate a region where several loops of the helix can be followed around the caudal flagella.

Movie S2

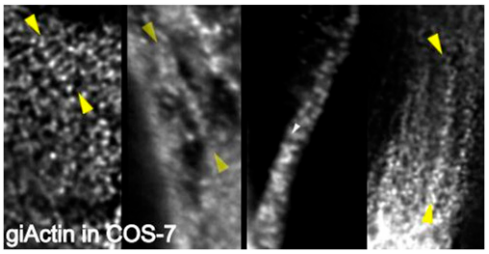

Movie S3. *Z*-series through COS-7 cells expressing giActin. Yellow arrowheads mark giActin helices. White arrowhead follows the path of one coil through the image stack.

Movie S3